

Neutron scattering study of the crystal electric field levels in an induced-moment spin-glass $\text{PrP}_{0.9}$

H. Yoshizawa and S. M. Shapiro

Brookhaven National Laboratory, Upton, New York 11973

S. K. Hasanain* and R. P. Guertin*

Tufts University, Medford, Massachusetts 02155

(Received 13 July 1982)

A neutron scattering study of the induced-moment spin-glass $\text{PrP}_{0.9}$ has been performed and the results compared with a singlet ground-state stoichiometric sample $\text{PrP}_{1.0}$. No magnetic order is observed in the polycrystalline samples down to $T=4.5$ K. The Γ_1 - Γ_4 crystalline electric field excitations observed in $\text{PrP}_{1.0}$ are decreased by 10% in $\text{PrP}_{0.9}$ which is in the opposite sense to that expected from changes in the lattice parameter. In addition, another broad excitation appears at low energies in $\text{PrP}_{0.9}$ which probably plays a role in inducing moments on Pr sites. The random distribution of these moments reflects the random vacancy distribution, and they give rise to the observed spin-glass behavior. The temperature dependence of the quasielastic intensity measured at small momentum transfer, $Q=0.14 \text{ \AA}^{-1}$, exhibits a peak at $T\sim 8$ K which is in agreement with the bulk susceptibility measurements.

I. INTRODUCTION

Spin-glass behavior has been observed in a number of randomly mixed compounds including both metals¹⁻³ and insulators,⁴ all of which show very similar bulk magnetic behaviors, such as a cusp in the bulk susceptibility⁵ and a frequency dependence of a peak in the ac susceptibility.^{3,6} There usually exist well-defined magnetic moments in such materials, and the spin-glass behavior is believed to result from the effective randomness of the exchange interaction acting between the magnetic moments. In the case of a dilute alloy spin-glass such as CuMn (Ref. 1) and AuFe ,² the random-exchange interaction is produced by the oscillatory character of the Ruderman-Kittel-Kasuya-Yosida (RKKY) interaction between randomly distributed magnetic moments (impurities). In the case of the insulating spin-glass, specifically in the case of $\text{Eu}_x\text{Sr}_{1-x}\text{S}$,⁴ the random-exchange interaction comes from the frustration between the ferromagnetic first-nearest-neighbor and the antiferromagnetic second-nearest-neighbor exchange interactions.

However, spin-glass behavior is not restricted to systems which have well-defined magnetic moments. An analogous phenomenon occurs in Stoner alloys such as RhCo ,⁷ where the spin fluctuations are too large for isolated impurity ions to carry well-defined magnetic moments. The existence of induced-moment spin-glass behavior is demonstrated by the experiments on the rare-earth ion-dilute alloy ScTb ,⁸

in which the solvent is a nonmagnetic metal and the solute ion has a singlet ground state in the host's crystalline electric field (CEF). Induced-moment spin-glass behavior is also observed in nonstoichiometric PrP_y ,^{9,10} which will be discussed in this paper. For this material, nonstoichiometry plays the pivotal role in introducing the spin-glass behavior.

Recently, Sherrington¹¹ proposed a theory for the induced-moment spin-glass. Combining a singlet-singlet model¹² for induced moments with the Edwards-Anderson-type model¹³ for spin-glasses, he discussed the induced-moment spin-glass behavior. His theory is characterized by three parameters: a CEF splitting Δ , a mean of the exchange interaction \mathcal{J}_0 , and the standard deviation of the exchange distribution \mathcal{J} . A ferromagnetic phase occurs if $z\mathcal{J}_0 > (\Delta/2\alpha^2)$, while a spin-glass phase occurs if $\sqrt{z}\mathcal{J} > (\Delta/2\alpha^2)$, where α is a matrix element between two singlet levels, and z is the coordination number of the lattice. The condition of $\mathcal{J} = \sqrt{z}\mathcal{J}_0$ gives a multicritical point and the occurrence of the spin-glass phase necessitates $\mathcal{J} > \sqrt{z}\mathcal{J}_0$.

In this paper we report on a neutron scattering study of the CEF excitations in nonstoichiometric $\text{PrP}_{0.9}$ and compare them with the stoichiometric $\text{PrP}_{1.0}$. Recently, a detailed study of the bulk magnetic properties of $\text{PrP}_{0.9}$ demonstrated the presence of spin-glass behavior¹⁰ (hereafter, this work is referred to as I.) Pure $\text{PrP}_{1.0}$ is a singlet ground-state Van Vleck paramagnet. An early neutron scattering

study concluded that the splitting between singlet and the first excited triplet ($\Gamma_1-\Gamma_4$) is 11.0 ± 1.0 meV (127 K).¹⁴ It was speculated in I that the deficiency of anion sites introduced by the nonstoichiometry partly removes the degeneracy of the CEF levels and induced moments appear at some sites, due to an overcritical admixture of excited states into the ground state. Because of the variation of the Pr-site local environments, the Pr moments are expected to vary from site to site. It was speculated that the RKKY interaction causes the effective-random interactions between induced moments, and this interaction is enhanced by an increased conduction-electron concentration accompanying the introduction of anion vacancies.¹⁵

Our purpose is to clarify the relationship between the spin-glass behavior and the CEF level structure in $\text{PrP}_{0.9}$. The advantages of adopting nonstoichiometric PrP_y samples are as follows. The CEF level structures of monpnictides have been studied extensively by neutron scattering and analyzed rather successfully with the point-charge model (PCM).¹⁴ Therefore, we can study the PrP_y by comparing the results with the well-studied pure $\text{PrP}_{1.0}$. The results of our experiment show that the speculations of I are indeed correct and the CEF scheme in $\text{PrP}_{0.9}$ are strongly modified by the presence of vacancies on the P site.

II. PRELIMINARY DETAILS

Nonstoichiometric PrP_y ($1.00 \geq y \geq 0.85$) is one of the monpnictides which show a wide range of solid solubility.¹⁶ The rocksalt structure is retained over all concentrations. As y decreases, the lattice constant a_0 decreases monotonically from $a_0 = 5.886 \text{ \AA}^{-1}$ for $y = 1.0$ to 5.855 \AA^{-1} for $y = 0.9$.⁹ From density measurements,¹⁷ it is concluded that the nonstoichiometry creates vacancies on anion sites. No vacancy structure is observed in these compounds. For GdP_y and GdS_y , the anion deficiency increases the conduction-electron concentration.¹⁵ For PrP_y , a similar increase of free-carrier density is expected. Because of the semimetallic character of PrP , this may drastically enhance the exchange interaction between Pr atoms which is presumably the RKKY interaction.

Figure 1 shows the bulk susceptibility of the samples used in the neutron scattering experiments. The measurements were performed in the same way as reported in I. Pure $\text{PrP}_{1.0}$ shows a Van Vleck susceptibility which is essentially independent of the temperature below 20 K. For $\text{PrP}_{0.9}$ the susceptibility is strongly enhanced and exhibits a peak near $T \sim 7.5$ K. The inset of Fig. 1 shows the magnetic moment σ versus applied field for $\text{PrP}_{0.9}$ and $\text{PrP}_{1.0}$

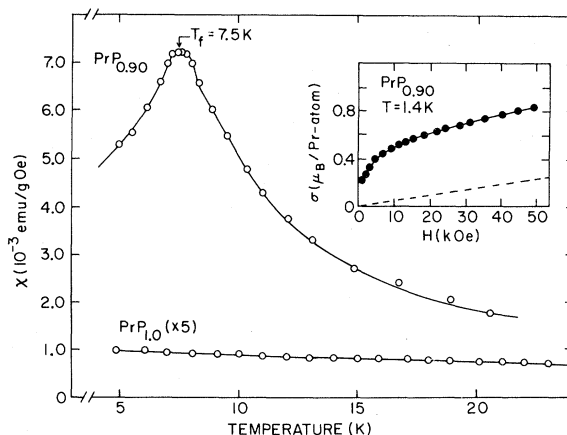


FIG. 1. Low-field ($H = 10$ Oe) susceptibility vs temperature for $\text{PrP}_{0.9}$ and $\text{PrP}_{1.0}$. Inset shows magnetization σ vs applied field H at $T = 1.4$ K.

(the dashed line) at $T = 1.4$ K. Compared with the Pr^{3+} saturated moment of $3.2\mu_B$ per Pr atom, $\text{PrP}_{0.9}$ exhibits a substantial magnetization at high fields. The large moment per Pr atom and the non-linearity of the magnetization curve indicate a moment on the Pr ion. Below 8.0 K we observed time-dependent remanence for $\text{PrP}_{0.9}$. As reported in I, a logarithmic decay of σ versus time is observed in the thermoremanent magnetization for those nonstoichiometric PrP_y samples which show spin-glass behavior. The peak in the temperature dependence of the ac susceptibility exhibits a frequency dependence over the range of $1 \text{ Hz} < f < 10^4 \text{ Hz}$. (However, for $f < 1$ Hz, the peak reaches a low-temperature limit and becomes independent of frequency.⁹) These features are common to many spin-glass materials.

To understand the induced-moment spin-glass, we need to know the CEF level structure. The effective PCM explains¹⁸ reasonably well the transitions among the CEF levels in pure PrP as well as most other rare-earth monochalcogenides and monpnictides.¹⁴ For rare earths at cubic-symmetry sites, the crystal-field Hamiltonian may be written:

$$\mathcal{H}_{\text{CEF}} = B_4 \chi_4 (O_4^0 + 5O_4^4) + B_6 \chi_6 (O_6^0 - 21O_6^4), \quad (1)$$

where the O_n^m are Stevens-operator equivalents and the χ_n are reduced matrix elements.¹⁸ In the PCM the coefficients B_4 and B_6 are given for the rocksalt structure by

$$B_4 = \frac{7}{16} (Ze^2/R^5) \langle r^4 \rangle (1 + \epsilon_4),$$

$$B_6 = \frac{3}{64} (Ze^2/R^7) \langle r^6 \rangle (1 + \epsilon_6), \quad (2)$$

where Ze is the effective charge at the ligand, R is

TABLE I. Probabilities of the vacancy distribution on six nearest-neighbor sites of Pr ions for PrP_y .

Number of vacancies n	Probabilities $P(n)^a$ for		
	$\text{PrP}_{1.0}$	$\text{PrP}_{0.9}$	$\text{PrP}_{0.85}$
0	1.00	0.531	0.377
1	0.0	0.354	0.399
2	0.0	0.0984	0.176
3	0.0	0.0146	0.0415
4	0.0	0.0012	0.0055
5	0.0	b	
6	0.0		

$$^a P(n) = \binom{6}{n} (1-y)^n y^{6-n}.$$

^bNegligibly small.

the separation of rare-earth ligands, and ϵ_4, ϵ_6 are small correction factors. For PrP and similar materials, the CEF level scheme is almost entirely due to the fourth-order term in Eq. (1).

In cubic symmetry the ninefold-degenerate $J=4$ ground-state multiplet of Pr^{3+} (3H_4) splits into four levels: $\Gamma_1(1)$, $\Gamma_4(3)$, $\Gamma_3(2)$, and $\Gamma_5(3)$ as shown in Fig. 2, where the number in parentheses indicates the degeneracy. The ground state is singlet and the $\Gamma_1 \rightarrow \Gamma_4$ splitting for $\text{PrP}_{1.0}$ is about 125 K so that it behaves like a singlet-triplet system at low temperatures.¹⁴

To see the effects of the anion deficiency on the CEF level structure, we performed point-charge model calculations assuming one or two vacancies.¹⁰ In the rocksalt structure, a Pr ion has six nearest-neighbor anions. The probability $P(n)$ that a Pr ion has n vacancies on its six nearest-neighbor anion sites is given by

$$P(n) = \binom{6}{n} (1-y)^n y^{6-n}, \quad (3)$$

where $y \leq 1$ is the P atom concentration and

$$\binom{6}{n} = \frac{6!}{(6-n)!n!}$$

is the combination factor. We tabulated the numerical values $P(n)$ for three different concentrations $y=1.0, 0.9$, and 0.85 in Table I. It is obvious that we can neglect the cases where the Pr ion has more than two neighboring vacancies.

The CEF level structures for one- and two-vacancy models are illustrated schematically in Figs. 2(a) and 2(b), respectively, where B_{40}^c is equal to B_4 in Eq. (2) and $B_{20} = Ze^2/R^3 \langle r^2 \rangle (1 + \epsilon_2)$. B_{20} is

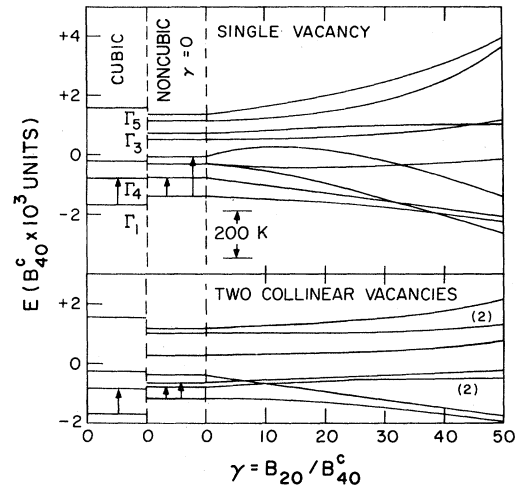


FIG. 2. (Upper panel) (a) Crystalline electric field (CEF) energy levels for Pr^{3+} in PrP_y for the case of one vacancy. (b) (lower panel) CEF energy levels for Pr^{3+} in PrP_y for the case of two collinear nearest-neighbor vacancies.

zero for $\text{PrP}_{1.0}$. The energy scale is illustrated on the left-hand side of Fig. 2. The parameter γ is the ratio of second- to fourth-order terms in the CEF Hamiltonian. We assume $B_{60}=0$, this being nearly the case for stoichiometric $\text{PrP}_{1.0}$. In Fig. 2(a) one can see a removal of the degeneracy of the excited levels and even the crossing with the ground state. Thus the vacancies created randomly on the anion sublattice must change the CEF level structure drastically. For low values of γ ($\gamma=50$) this results in a smaller gap between the singlet ground state and the first excited state, and can even result in a magnetic ground state for some Pr ions.

III. EXPERIMENTAL RESULTS AND ANALYSIS

Neutron scattering experiments were carried out on a triple-axis spectrometer at the High Flux Beam Reactor at Brookhaven National Laboratory. The spectrometer was operated in a triple-axis configuration with pyrolytic graphite monochromator and analyzer. The $\theta - 2\theta$ scans were performed with an incident neutron energy of 14.7 or 40.5 meV, while the inelastic scattering experiments were performed mainly with a fixed analyzer energy of 14.7 meV. The horizontal collimations throughout the spectrometer were all 40 min and a pyrolytic graphite filter was placed after the monochromator crystal to eliminate higher-order contaminations.

Samples used in our experiments were prepared in the same manner described in I, and were ground to a powder. The homogeneity of the powdered sam-

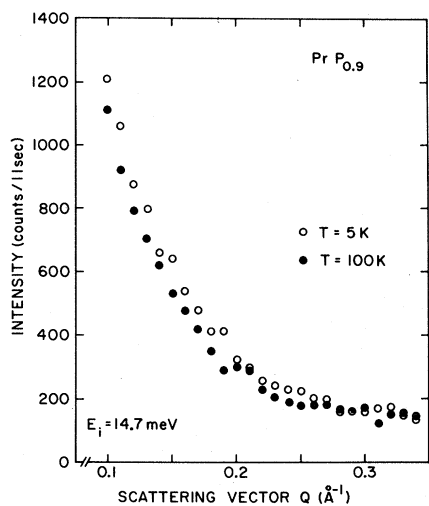


FIG. 3. Powder profile in the small scattering vector region at $T = 5$ K (open circles) and at $T = 100$ K (closed circles) for $\text{PrP}_{0.9}$.

ples was checked by the rocking curve of the (200) nuclear Bragg reflection. The reflected intensity showed no measurable dependence on the rocking angle.

Firstly, the powder patterns were measured with the scattering vector varying from $Q = 0.1$ to $Q = 4.1 \text{ \AA}^{-1}$ at two different temperatures, $T = 5$ and 100 K, for both pure $\text{PrP}_{1.0}$ and nonstoichiometric $\text{PrP}_{0.9}$. No long-range magnetic ordering was observed in either sample. The main difference between the two samples was an increase of the diffuse scattering intensity for $\text{PrP}_{0.9}$ at 5 K for $Q \lesssim 0.3 \text{ \AA}^{-1}$. A portion of the powder pattern of $\text{PrP}_{0.9}$ for $0.1 \text{ \AA}^{-1} \leq Q \leq 0.34 \text{ \AA}^{-1}$ is shown in Fig. 3. The increase of the intensity for $Q \lesssim 0.25 \text{ \AA}^{-1}$ comes from the background of the forward scattering due to the finite- Q resolution. A similar Q -dependent background is also observed in pure $\text{PrP}_{1.0}$, but there is no temperature dependence from $T = 5$ to 200 K. In the case of $\text{PrP}_{0.9}$, however, one can clearly see the increase of the scattering intensity at $T = 5$ K from Fig. 3. We first monitored the temperature dependence at $Q = 0.14 \text{ \AA}^{-1}$ with the spectrometer set for zero energy transfer and found that the intensity decreased monotonically on elevating the temperature from 5 to 30 K. Since the energy resolution was 0.9 -meV full width at half maximum (FWHM), we suspected that the energy resolution was too good to properly integrate over the quasielastic scattering. We therefore changed the incident neutron energy from $E_i = 14.7$ to 40.5 meV which gives an energy resolution of about 4.2 meV FWHM, and observed temperature dependence as shown in Fig. 4. The intensity from $\text{PrP}_{0.9}$ exhibits a peak of $T \sim 8$ K and decreases at higher temperatures, whereas the inten-

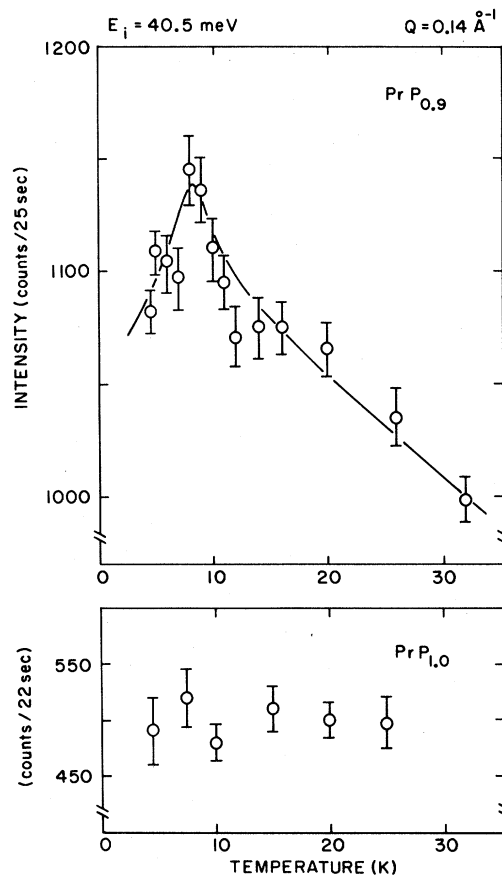


FIG. 4. Temperature dependence of the quasielastic scattering intensity for $\text{PrP}_{0.9}$ and $\text{PrP}_{1.0}$.

sity from pure $\text{PrP}_{1.0}$ shown in the lower part of Fig. 4 remains constant over the temperature region studied. These results are in excellent agreement with the bulk susceptibility shown in Fig. 1. Therefore, we believe that the quasielastic intensity appearing in the small- Q region at low temperatures reflects the spin-glass behavior of nonstoichiometric $\text{PrP}_{0.9}$.

In order to study the relation between the spin-glass behavior and the CEF level structure of PrP_y , we observed the excitations between the CEF levels at the scattering vector Q of 1.3 , 2.4 , and 5.0 \AA^{-1} . In Fig. 5 we show the temperature dependence of the inelastic neutron scattering profiles for both $\text{PrP}_{1.0}$ and $\text{PrP}_{0.9}$ observed at $Q = 1.3 \text{ \AA}^{-1}$. Since the thermal populations of the excited levels are negligible at $T \sim 5$ K, we observe only the transitions from the ground state to the excited levels. For pure $\text{PrP}_{1.0}$ a transition from the singlet ground state Γ_1 to the first excited triplet Γ_4 appears at around 11 ± 0.5 meV which is in good agreement with the early time-of-flight measurements.¹⁴ Another peak seen at $E = 0$ meV results from the nuclear spin in-

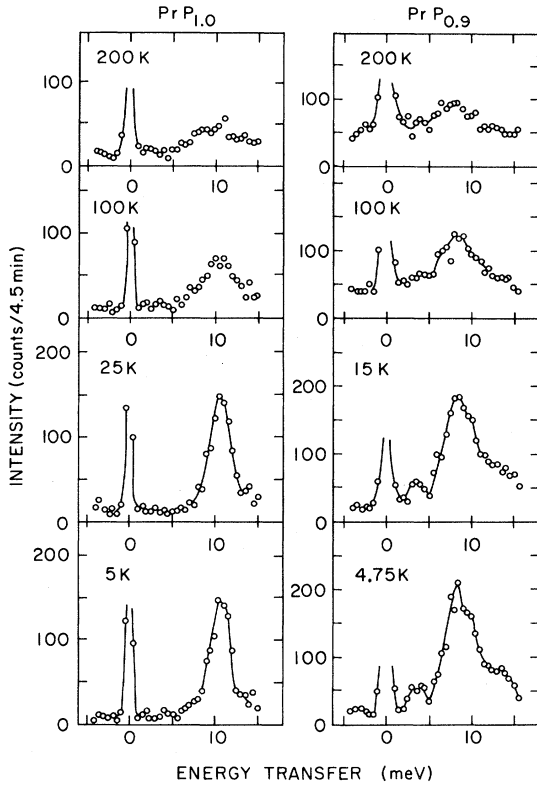


FIG. 5. Temperature dependence of the inelastic scattering profiles from $\text{PrP}_{0.9}$ (right) and $\text{PrP}_{1.0}$ (left).

coherent scattering whose width of about 1.0 meV gives the energy resolution of the present scans. The width of the $\Gamma_1 \rightarrow \Gamma_4$ transition is broadened possibly because of the average of the dispersion effect by the exchange interaction in the powdered sample. On increasing the temperature its intensity decreases due to the decrease of the thermal population of the ground state, while the transition from Γ_4 to Γ_3 appears at about 8 meV.

On the other hand, the excitation spectra of nonstoichiometric $\text{PrP}_{0.9}$ differs drastically from that of stoichiometric $\text{PrP}_{1.0}$. At low temperatures there appear several peaks at $\Delta E \sim 4, 8, 10,$ and 14 meV. As mentioned earlier, at low temperatures only the ground state is occupied, so that the excitation spectra shown in the lowest panels immediately give the energy splitting between the ground state and the excited levels. Therefore, it is clear that the anion deficiency of 10% changed the CEF level structure significantly. These results may be explained by the superposition of the pure cubic model, the one-vacancy model, and presumably the two-vacancy model with suitable weights as discussed in Sec. II.

The scattered neutron intensity for the CEF transitions allowed by the Hamiltonian (1) may be written¹⁹

$$I(\omega) = e^{-2W} \left[\frac{1.91e^2}{2mc^2} g_J \right]^2 \frac{k}{k_0} F^2(Q) \times \sum_{nm} \rho_m |\langle n | J_{\perp} | m \rangle|^2 \delta \left[\frac{E_n - E_m}{\hbar} - \omega \right], \quad (4)$$

where the symbols have their usual meaning and $|n\rangle$ and $|m\rangle$ are the eigenstates of a given J multiplet. Transitions from levels $|m\rangle$ to $|n\rangle$ occur at an energy difference $(E_n - E_m)$. ρ_m denotes the thermal population of the initial state, so that the CEF excitations obey the Boltzmann statistics. For the present case, where the nonstoichiometry lifts the degeneracies, the neutron scattering intensities were calculated in the following way: First the CEF Hamiltonian for zero, one, and two vacancies was diagonalized and the perturbed eigenfunctions determined. Next the J_{\perp} matrix elements were calculated between the states. Finally, the $P(n)$ were used to weight the transition probabilities in order to give the total scattered intensity $I(\omega)$. $I(\omega)$ for $\text{PrP}_{0.9}$ is then given by the following superposition:

$$I_{0.9}(\omega) = 0.531I_{0v}(\omega) + 0.354I_{1v}(\omega) + 0.098I_{2v}(\omega) + \dots, \quad (5)$$

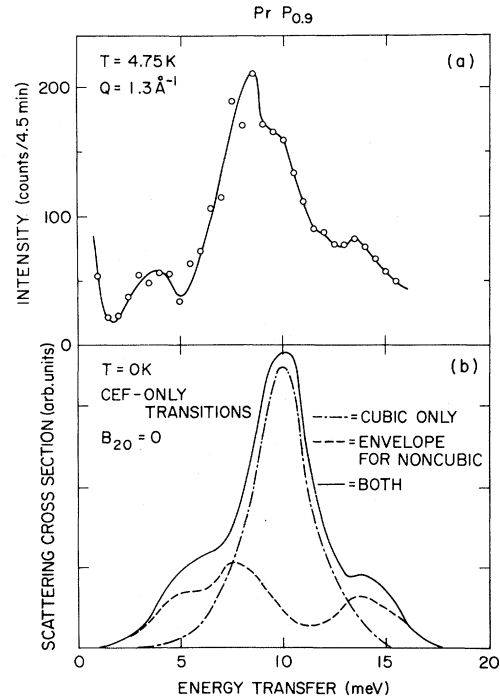


FIG. 6. (a) Inelastic scattering profiles from $\text{PrP}_{0.9}$ observed at $Q = 1.3 \text{ \AA}^{-1}$ at $T = 4.75 \text{ K}$. (b) Transition probabilities $|\langle m | J_{\perp} | n \rangle|^2$ for $\text{PrP}_{0.9}$ assuming $\gamma = B_{20}/B_{40}^c = 0$ at $T = 0 \text{ K}$, where the instrumental width of energy resolution is folded.

where $I_{0v}(\omega)$ is the spectrum expected for zero vacancies and $I_{1v}(\omega)$ and $I_{2v}(\omega)$ are the spectra expected from the one- and two-vacancy models, respectively.

The results of these calculations for $\gamma(B_{20}/B_{40}^c)=0$ at $T=0$ K and the corresponding low-temperature spectra for $\text{PrP}_{0.9}$ are shown in Fig. 6 in the same energy scale. Although the intensity of the zero vacancy line at $\hbar\omega \sim 10$ meV is about four times too large, the positions and relative strengths of the other transitions bear a very close resemblance to the observations.

Peaks seen at ~ 4.0 , ~ 8.0 , and ~ 14.0 meV result from the transitions in the one-vacancy model for $\gamma \leq 50$, while the peak at ~ 10.0 meV can result from the $\Gamma_1 \rightarrow \Gamma_4$ transition in the cubic model, the energy being shifted to some extent by the smaller lattice constant in the nonstoichiometric sample (discussed in Sec. IV.) However, the fact that this shift is not large suggests that the effective anion charge for $\text{PrP}_{0.9}$ is close to that of $\text{PrP}_{1.0}$. Because of the rather large ambiguity of the complicated CEF level structure, no further attempt was made to analyze the observed temperature dependences. In the following section we shall discuss the possible origin of the spin-glass behavior in PrP_y .

IV. DISCUSSION

The influence of the anion deficiency on the Pr ion is a change of the CEF level structure of Pr ions due to the lower symmetry, the decrease of the gap Δ due to the decrease of the lattice parameter a_0 , and an increase of the conduction-electron concentration.¹⁰ All of these have important effects on the spin-glass behavior of PrP_y . As seen in Fig. 6, the peak at $\Delta E \sim 4$ meV indicates symbolically the change of the CEF level structure of Pr ions. Following the discussion given in Sec. III, we can expect that about 35% of the Pr atoms have one vacancy as their nearest-neighbor sites and thus behave like a singlet-singlet system (Fig. 2). In addition, the magnitude of the gap Δ decreases from 11 to 4 meV for some Pr ions, so that moments are more easily induced than in pure $\text{PrP}_{1.0}$. A probable interpretation of our results is that the nondegenerate excited levels in the one-vacancy model may cause the excitations at 4, 8, and 14 meV, while the $\Gamma_1 \rightarrow \Gamma_4$ transition of 53% Pr ions with purely cubic symmetry is superposed at $\Delta E \sim 10$ meV. In this interpretation the spin-glass behavior is explained by the mixing of the ground state and the first excited level at 4 meV. Simple theory¹¹ predicts that the transition between these levels goes soft when the moments are induced. In fact, the softening accompanied by the induced-moment antiferromagnetism in PrSb was

observed by neutron scattering experiments,²⁰ although the softening of the transition frequency was rather inadequate. PrSb behaves as a singlet-singlet system at low temperature because the degeneracy of the first excited triplet Γ_4 is lifted near the X point due to the anisotropy of the exchange interactions.²⁰ For PrSb the application of high pressure caused the decrease of the gap Δ . Therefore, on increasing the pressure, PrSb satisfies the condition $z\mathcal{J}_0 > (\Delta/2\alpha^2)$.²⁰

In the case of $\text{PrP}_{0.9}$ the vacancies lift the degeneracy of the triplet Γ_4 so as to result in the behavior of the singlet-singlet model. However, what we observe is not a softening but an anomaly of the intensity of quasielastic scattering at small momentum transfers. Because the spin-glass transition has no particular q value where the singularity appears in the physical quantities, it does not necessitate the softening of the 4-meV line at $T_f \sim 8$ K. On the contrary, it is presumably hidden by the spin-glass feature even if the softening really occurs.

Another possible mechanism for the peak of the quasielastic scattering is the intra- Γ_4 transition of 53% Pr ions in the cubic symmetry. A typical example of this case is given by Pr_3Ti ,²¹ where the $\Gamma_1 \rightarrow \Gamma_4$ transition exhibits little temperature dependence. Detailed theoretical analysis²² showed that the $\Gamma_1 \rightarrow \Gamma_4$ transition remains the so-called "hard mode" at the ferromagnetic phase transition and that only the intratriplet quasielastic mode shows the anomaly, which was confirmed later by neutron scattering experiments. For pure $\text{PrP}_{1.0}$, the exchange interactions between Pr atoms are too weak to drive the ferromagnetic ordering with the anomaly of the quasielastic scattering [i.e., $z\mathcal{J}_0 \ll (\Delta/\alpha^2)$]. For nonstoichiometric $\text{PrP}_{0.9}$, however, the smaller lattice parameter favors the decrease of the gap Δ , and the anion deficiency may cause the drastic enhancement of the exchange interactions, perhaps through increased conduction-electron concentration. Therefore, the intratriplet transition might be responsible for the temperature dependence of the quasielastic intensity for $\text{PrP}_{0.9}$. In any event, our results are consistent with the known behaviors of the singlet ground-state materials.

We would like to point out the importance of the conduction electrons. The origin of the exchange interactions between Pr atoms may be the RKKY interactions mediated by the conduction electrons. In the case of PrP_y , the vacancies probably change the number of free carriers drastically. The existence of this phenomenon was clearly demonstrated by Hall effect data in $\text{GdP}_y\text{-GdS}_y$.¹⁵ This suggests that the exchange will be affected by anion differences.

Our results shown in Fig. 5 indicate the $\Gamma_1 \rightarrow \Gamma_4$

transition line is shifted slightly towards lower energy consistent with studies of PrSb at high pressure.²⁰ These results contradict the prediction of the PCM even qualitatively. The failure of the PCM in this regard was pointed out at first from the studies of the pressure effects²³ on the NMR Knight shift and the susceptibility, where the cause of the unusual pressure dependence was attributed to the change of either the gap or the exchange or both. For pure PrP_{1.0}, a study of the temperature dependence of the Knight shift on the pressure²⁴ leads to the conclusion that the results cannot be explained by taking account of the temperature dependence of the exchange interactions. Clearly, the pressure cannot change the CEF symmetry of Pr ions, so that χ_n and R in Eqs. (1) and (2) depend only weakly on the pressure. Therefore, Weaver and Schirber²⁴ conjectured that when phenomena with the constant conduction-electron-concentration character are observed, the PCM is valid, whereas when the concentration of the conduction electrons is changed during the observations, the PCM based on the tight-binding electron picture fails to account for the results, presumably due to the screening of the CEF. Because the conduction-electron concentration in PrP_y is changed, we do not expect PCM predictions to be closely followed.

Another interesting feature of the data and one which tends to substantiate the inadequacy of the PCM is the values of the parameter $\gamma (=B_{20}/B_{40}^c)$ at which the calculated energy splittings of the CEF levels appear to match the experimentally observed transitions. PCM predicts values of $\gamma \sim 1800$, but the transition energies would be 2 orders of magnitude too high. For such large splittings, induced moments would be practically impossible. As seen from Figs. 2 and 6 all the observed transitions can

be accounted for with values of γ in the range $0 \leq \gamma \leq 50$. The inconsistency of the results with higher γ values suggests that other mechanisms besides those considered in the bare PCM are active and these have the effect of drastically reducing the B_{20} term in the CEF Hamiltonian while affecting the B_{40} term to a much lesser extent.

In conclusion, the anomaly of the quasielastic scattering in the small momentum region is consistent with the bulk susceptibility. The change of the CEF level structure is accounted for at least semiquantitatively by a simple model using nearest-neighbor vacancies. The CEF excitations in PrP_{0.9} are unaffected by the spin-glass ordering of the Pr moments. The probable mechanism to induce moments in PrP_{0.9} is the mixing of the ground state with the lowest excitation level which results from a change of the CEF schemes due to the removal of the cubic symmetry by the defect nature of the compound. In addition, the shift in the zero vacancy line of PrP_{0.9} to the lower energy side is consistent with the results of other experiments on the singlet ground-state materials, including PrP_{1.0} in which the physical quantities related to the decrease of the effective lattice constant were studied. This behavior is in contradiction to the PCM which predicts that a decrease of the lattice parameter should cause an increase of the level splitting.

ACKNOWLEDGMENTS

The work at Brookhaven was supported by the Division of Materials Sciences, U.S. Department of Energy, under Contract No. DE-AC02-76CH00016. The work at Tufts was supported by a NSF Grant No. DMR80-10530, and by the NSF at the Francis Bitter National Magnet Laboratory.

*Visiting scientist appointment at the Francis Bitter National Magnet Laboratory, M.I.T., Cambridge, MA 02139.

¹R. W. Kaitler, J. S. Kouvel, and H. Claus, *J. Magn. Mater.* **5**, 356 (1977); E. M. Gray, *J. Phys. F* **9**, L167 (1979).

²C. N. Guy, *J. Phys. F* **7**, 1505 (1977); **8**, 1309 (1978).

³H. V. Lohnneisen, J. L. Tholence, and R. Tournier, *J. Phys. (Paris)* **39**, C6-922 (1978); H. V. Lohnneisen and J. L. Tholence, *J. Magn. Mater.* **15-18**, 171 (1980).

⁴F. Holtzberg, J. L. Tholence, H. Godfrin, and R. Tournier, *J. Appl. Phys.* **50**, 1717 (1979); K. Westerholt, U. Scheer, and S. Methfessel, *J. Magn. Mater.* **15-18**, 823 (1980); H. Maletta and W. Felsh, *Phys. Rev. B* **20**, 1245 (1979).

⁵L. E. Wenger and P. H. Keeson, *Phys. Rev. B* **11**, 3497

(1975).

⁶G. Zibold, *J. Phys. F* **8**, L229 (1978); J. L. Tholence, *Solid State Commun.* **35**, 113 (1980).

⁷B. R. Coles and H. D. Jamieson, in *Low Temperature Physics—LT 13*, edited by K. D. Timmerhaus, W. J. O' Sullivan, and E. F. Hammel (Plenum, New York, 1974), Vol. 2, pp. 414–416.

⁸B. V. B. Sarkissian and B. R. Coles, *Commun. Phys.* **1**, 17 (1976); B. V. B. Sarkissian, *J. Phys. F* **7**, L139 (1977).

⁹K. Westerholt and S. Methfessel, *Physica (Utrecht)* **86-88B**, 1160 M. Guyot, S. Foner, S. K. Hasanain, R. P. Guertin, and K. Westerholt, *Phys. Lett.* **79A**, 339 (1980).

¹⁰S. K. Hasanain, R. P. Guertin, K. Westerholt, M. Guyot, and S. Foner, *Phys. Rev. B* **24**, 5165 (1981).

- ¹¹D. Sherrington, *J. Phys. C* **12**, L929 (1979).
- ¹²G. T. Trammel, *J. Appl. Phys.* **31**, 362S (1960); *Phys. Rev.* **131**, 932 (1963).
- ¹³D. Sherrington, *J. Phys. C* **8**, L208 (1975); B. W. Southern, *J. Phys. C* **9**, 4011 (1976); M. W. Klein, *Phys. Rev. B* **14**, 5008 (1976).
- ¹⁴K. C. Turberfield, L. Passell, R. J. Birgeneau, and E. Bucher, *J. Appl. Phys.* **42**, 1746 (1971); R. J. Birgeneau, E. Bucher, J. P. Maita, L. Passell, and K. C. Turberfield, *Phys. Rev. B* **8**, 5345 (1973).
- ¹⁵P. Wachter, E. Kaldis, and R. Hauger, *Phys. Rev. Lett.* **40**, 1404 (1978).
- ¹⁶E. Franceshi and J. L. Olcese, *J. Phys. Chem. Solids* **30**, 903 (1969).
- ¹⁷G. Buzzone and G. L. Olcese, in *Propriétés Thermodynamiques, Physiques et Structurales des Dérivés Semi-Métalliques* (CNRS, Paris, 1965), p. 387.
- ¹⁸K. W. H. Stevens, *Proc. Phys. Soc. London, Sect. A* **65**, 209 (1952); M. T. Hutchings, *Solid State Phys.* **16**, 227 (1964); K. R. Lea, M. J. M. Leask, and W. P. Wolf, *J. Phys. Chem. Solids* **23**, 1381 (1962).
- ¹⁹P. G. de Gennes, in *Magnetism*, edited by G. T. Rado and H. Suhl (Academic, New York, 1963), Vol. 3, p. 115.
- ²⁰C. Vettier, D. B. McWhan, E. I. Blount, and G. Shirane, *Phys. Rev. Lett.* **39**, 1028 (1977); D. B. McWhan, C. Vettier, R. Youngblood, and G. Shirane, *Phys. Rev. B* **20**, 4612 (1979).
- ²¹R. J. Birgeneau, J. Als-Nielsen, and E. Bucher, *Phys. Rev. Lett.* **27**, 1530 (1971); R. J. Birgeneau, in *Magnetism and Magnetic Materials—1973 (Boston, Massachusetts)*, Proceedings of the 19th Annual Conference on Magnetism and Magnetic Materials, edited by C. D. Graham and J. J. Rhyne (New York, 1973), p. 1664; J. Als-Nielsen, J. K. Kjems, W. J. L. Buyers, and R. J. Birgeneau, *J. Phys. C* **10**, 2673 (1977).
- ²²S. R. P. Smith, *J. Phys. C* **5**, L157 (1972).
- ²³H. T. Weaver and J. E. Schirber, in *Magnetism and Magnetic Materials—1974 (San Francisco, California)*, Proceedings of the 20th Annual Conference on Magnetism and Magnetic Materials, edited by C. D. Graham and G. H. Lander, (AIP, New York, 1974), p. 49; R. P. Guertin, J. E. Crow, L. D. Longinotti, E. Bucher, L. Kupferberg, and S. Foner, *Phys. Rev. B* **12**, 1005 (1975).
- ²⁴H. T. Weaver and J. E. Schirber, *Phys. Rev. B* **14**, 951 (1976).